Journal of Engineering Physics and Thermophysics, Vol. 82, No. 2, 2009

HYDRODYNAMIC THEORY OF THE "STRUYA" FORMER-FLOWMETER

V. P. Starikov[a] **and N. A. Vladimirova**[b]

UDC 53.082.25,532.57,519.6,681.121

We have formulated the fundamentals of the hydrodynamic theory of the "Struya" former-flowmeter — a device for measuring the fluid flow rate and forming a homogeneous flow and a representative sample for subsequent qualitative analysis of the fluid medium composition. On the basis of the numerical solution of the Navier–Stokes equations, computer simulation of the flow of a viscous medium in the "Struya" former has been carried out. Models of homogeneous flow of a single incompressible fluid and of inhomogeneous flow of a two-phase dispersive fluid have been considered. Numerical calculations have confirmed the high characteristics of the "Struya" former which, as compared to the standard restrictions, has the lowest level of hydraulic losses and the highest accuracy of differential pressure formation.

Keywords: *flowmeter, former, restriction, computer simulation, hydraulic losses, dispersive medium.*

Introduction. To measure the velocity and flow rate of substances, flowmeters based on different principles of operation are used [1]. In the general case, measuring the flow rate and the quantity of a fluid or a gas is a rather difficult task, since the readings of the instruments are influenced by the physical properties of the flows being measured.

Variable differential pressure flowmeters are represented by restrictions. The operation of these flowmeters is based on the appearance of differential pressures on the restriction in the pipe when a fluid or a gas flows through it.

The specifications for the standard restrictions (diaphragms, nozzles, Venturi nozzles, Venturi tubes) having certain hydrodynamic features and metrological possibilities have been registered in State Standard [2]. For instance, the accuracy of measuring the flow rate by diaphragms strongly depends on the quality of their setting and the presence in front of them of parts of tubes of calculated diameter without additional disturbance sources. The chief disadvantage of the diaphragm is the high hydraulic resistance and considerable losses of head and working pressure. The accuracy of measuring the flow rate by nozzles is somewhat higher due to the absence of the additional error caused by the insufficient sharpness of the inlet edge and stalling phenomena in the "submerged" jet, but the loss of head in them is a little less than in diaphragms, and their manufacture is much more complicated. The direct loss of the working pressure in Venturi tubes in the general case is from 5 to 20%. Statistics shows that the error in measuring the flow rate by restrictions with the fulfillment of the requirements on lengths of rectilinear parts of pipes is no less than 1.5%. Moreover, there are problems with measurements of "low" flow rates. Attaining a higher accuracy in measuring the flow rate by the above standard restrictions is very problematic. The low accuracy of the formation and measurement of the differential pressure by these devices is explained by the fact that they are "submerged" in the flow and have the so-called "open" outlet — outflow of a liquid or gas jet into a "submerged" space which is the mainstream flow in the pipeline. At the interface between the "submerged" jet and the main stream there appear mixing layers and separation zones in which the effects of turbulent mixing and interaction of the flows prevail. These effects are casual and nonstationary in nature. For restrictions with an "open" outlet and a "submerged" jet, the influence of the arising stalling phenomena on the accuracy of the differential pressure formation is very difficult to evaluate. Clearly, direct pressure losses for "submerged" jets are very significant.

In the series of standard restrictions, a special place is occupied by the new flowmeter — the "Struya" former being developed [3, 4]. It is cut directly in the pipe and has no "open" outlet. The constructional arrangement of the

[a]OOO NPP "Vysokie Inzhenernye Tekhnologii" (Scientific-Production Limited Company "High Engineering Technologies"), Moscow, Russia; [b]Prof. N. E. Zhukovskii Central Aerohydrodynamic Institute, 1 Zhukovskii Str., Zhukovskii, Moscow Region, 140180, Russia; email: vlana@progtech.ru. Translated from Inzhenerno-Fizicheskii Zhurnal, Vol. 82, No. 2, pp. 308–319, March–April, 2009. Original article submitted November 19, 2007; revision submitted September 23, 2008.

1062-0125/09/8202-0303

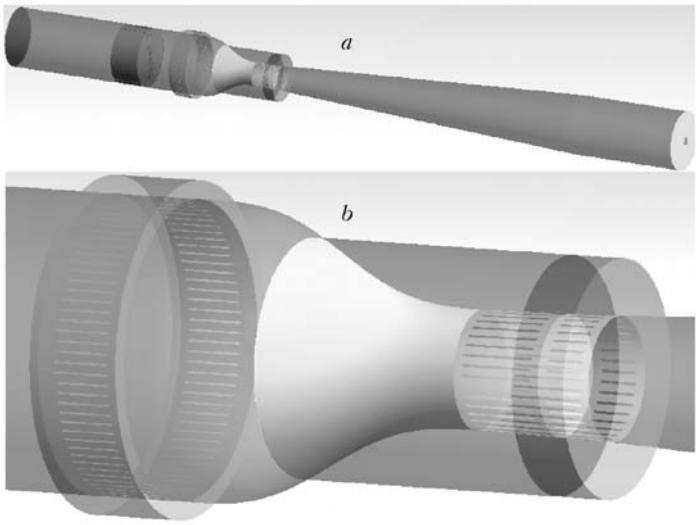

Fig. 1. Electronic three-dimensional solid-state geometrical model of the "Struya" flowmeter: a) complete geometry; b) fragment of the geometry in the nozzle region.

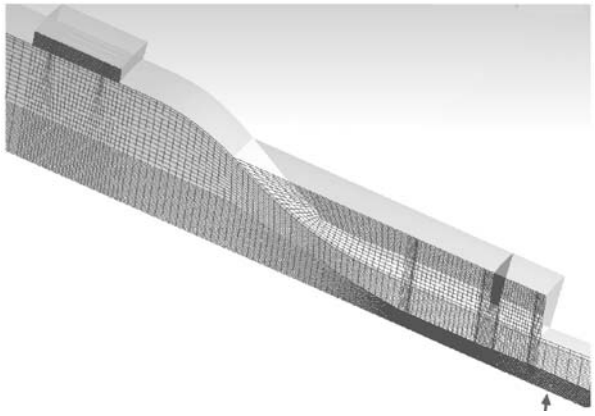

Fig. 2. Fragment of the computational grid in the periodic symmetry plane of the model.

"Struya" former makes it possible to separate and quantitatively estimate the processes proceeding directly in the zone of differential pressure formation.

The results presented are a continuation and generalization of our results published in [5–15].

Equipment and Software. Computer simulation of the hydrodynamics of a viscous incompressible fluid flow in the "Struya" flowmeter-former was carried out in the ANSYS/CFX, Ansys Inc* certified licensed program package. The construction of the three-dimensional geometrical CAD model of the former, the generation of computational grids, and the construction of the mathematical model of the former were carried out on an Intel Pentium 4 CPU 2.0 GHz personal computer with a RAM capacity of 2 Gb in a Windows 2000 environment. Hydrodynamic calculations have been made on two-core personal computers with a CPU of 2.6 GHz and 3.2 GHz (Intel(r) Core(tm) 2 Duo and Intel Pentium-D processors, respectively) with a RAM capacity of 4 Gb and 2 Gb, as well as on a cluster system of six units interconnected by a Gigabit Ethernet net interface controlled by a Linux SuSE10.0 ×86_64 operating system.

Geometrical Model and Computational Grids. Figure 1 shows the complete electronic three-dimensional solid-state geometrical model of the "Struya" flowmeter (Fig. 1a) and its fragment in the nozzle zone (Fig. 1b).

The single fluid flow in the former is axially symmetric (without account for the mass forces). Therefore, we used for the calculations a 20^{o} cylindrical sector whose angular size was determined by the constructional features of the

*License No. 408647.

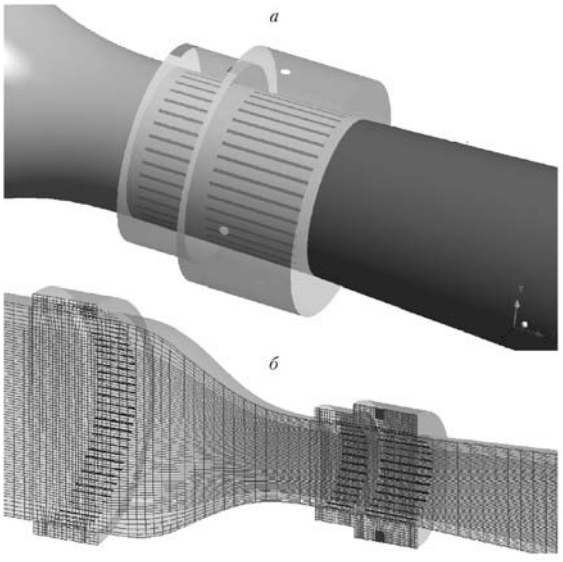

Fig. 3. "Struya" former: a) fragment of the geometry in the region of the nozzle and the pressure tap chamber; b) fragment of the computational grid in the vertical symmetry plane.

nozzle and the pressure and sampling chambers (minimal required number of longitudinal slots, etc.). Inside the calculation domain, a hexahedral spatial grid consisting of 600,000 computational nodes was generated. A fragment of the computational grid in one of the two planes of periodic symmetry bounding the calculated volume is given in Fig. 2.

The flow of a two-phase fluid with finely dispersed impurities requires taking into account the gravity forces. In this case, there is a vertical symmetry plane of the problem; therefore, for the calculation domain we used half of the complete three-dimensional model of the former, i.e., the 180^{o} sector, inside of which a hexahedral grid containing 1 million nodes was generated. Figure 3 shows a fragment of the geometrical model of the "Struya" former in the region of the nozzle and the sampling chamber with four round holes (Fig. 3a), as well as a fragment of the computational grid in the vertical symmetry plane (Fig. 3b).

In generating computational grids, we also used the original algorithms for constructing and adapting grids [16–19] developed by us for two- and three-dimensional problems of mathematical physics and computational dynamics of fluids.

Formulation of the Problem and Calculation Parameters. Consider a fluid medium as a single viscous incompressible fluid with a certain set of values of the main physical parameters and the results of simulating multiphase nonhomogeneous flows from the point of view of the model of fluid pairs (main fluid + finely dispersed fluid impurity).

We included in the calculations the following values and ranges of values of parameters of the physical properties of the fluid and hydrodynamic characteristics of the flow: the kinematic viscosity of the medium (e.g., oil) ν = 50–200 cSt, the fluid density ρ = 800–950 kg/m^3, the molar mass M = 220 kg/kmole, the specific heat capacity C_p = 1965 J/(kg·^{o}C), the heat conductivity coefficient λ = 0.134 W/(m·^{o}C), the working pressure P_{work} = 40–150 atm, the flow velocity V = 1.0–2.5 m/sec, the fluid temperature at the former inlet T = 10–50^{o}C.

In accordance with these values of parameters, the range of values of Reynolds numbers calculated for the inlet diameter of the former D = 0.8 m was Re = $4\cdot10^3$–$4\cdot10^4$. The level of the initial turbulence of the flow at the former inlet was assumed to be 1%.

Results of the Computer Simulation of a Homogeneous Flow. Within the framework of the ANSYS/CFX program package, we solved numerically the Reynolds-averaged Navier–Stokes equations (RANS) describing viscous laminar and turbulent flows of compressible and incompressible fluids and gases. Calculations were made on the basis of the finite-volume method with the use of a high-order numerical scheme for convective and viscous terms and an SST (Shear-Stress-Transport) k–ω-model [20] that permits simulating the wall turbulent boundary layer and regions of the turbulent flow with reverse eddy currents and separation zones. To reach convergence and obtain a stable stationary solution for one regime (all inlet and outlet parameters are fixed), it was required to carry out 100–200 iterations

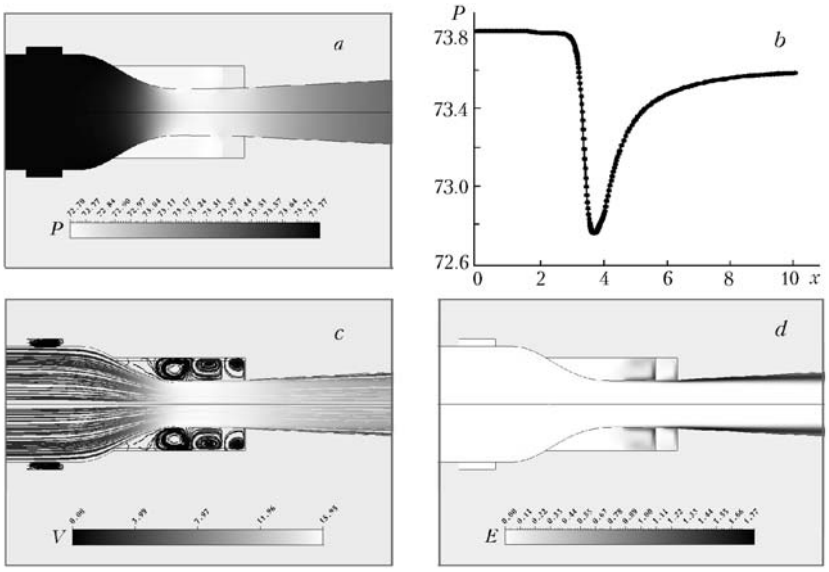

Fig. 4. Results of the numerical simulation of a homogeneous flow at the following values: ν = 200 cSt, K = 1.0 m^{-1}, ρ = 875 kg/m^3, T = 10°C, V = 2.5 m/sec; a) pressure field; b) pressure distribution along the former axis; c) pattern of streamlines; d) kinetic energy field of turbulent pulsations. E, m^2/sec^2; x, m; V, m/sec; P, atm.

on average. For the computational grid having about 600,000 nodes or 1 million nodes, it corresponded to 5–10 h of operation of the central processor of an Intel Pentium 4 personal computer.

From the results of the numerical simulation the distributed and summed hydrodynamic characteristics (static and total pressure fields, temperature and velocity fields, energies of turbulent pulsations, the structure of streamlines, values of hydraulic losses along the former path, etc.) were determined.

Figure 4 presents the results of the calculation of the pressure fields (Fig. 4a, b), streamlines (Fig. 4c), and kinetic energy of turbulent pulsations (Fig. 4d) for one set of kinematic and dynamic parameters of the problem under consideration. The fluid is assumed to be incompressible, viscous, and heat-conducting. For the incompressible fluid the level of the working pressure given in the calculations as the boundary condition at the former outlet does not influence the laws of pressure distribution along the former channel. The calculations have been made for the working gauge pressure P_{work} = 75 atm. The functional dependence of the kinematic viscosity of the fluid on the temperature $\nu(T)$ is often unknown, but it is known that the viscosity coefficient of the fluid decreases with increasing temperature. Figure 4 shows the calculated data for the "boundary" values of these quantities from the range under consideration: T = 10°C and ν = 200 cSt.

The honeycomb placed ahead of the former nozzle to homogenize the velocity field of the incoming fluid flow was modeled by a portion of a virtual porous material with given fluid pressure losses in it in the form of the dependence $dP/dx = -K\rho V^2/2$, where the loss factor K was taken equal to K = 0.07–1.0 m^{-1} in the range of kinematic viscosities ν = 50–200 cSt.

The parametric calculations performed by the authors cover the entire investigated range of variation of the problem parameters and give complete information about the features and characteristics of the flow. The calculations have shown that throughout the given range of variation of the problem parameters inside the former contour, the pressure chamber, and the sampling chambers, a stable stationary fluid flow with a low level of hydraulic losses along the full length of the channel (0.06–0.35% of the working pressure of 75 atm) is formed, which makes it possible to determine with a high accuracy (0.05–0.15%) the pressure and velocity in the core of the fluid flow in the nozzle by pressure measurements in the pressure tap chamber.

The formulated conclusions form the basis for the *hydrodynamic theory* of the "Struya" former. The presence of a fairly small but nonzero error in determining the flow parameters and the differential pressure in the nozzle from

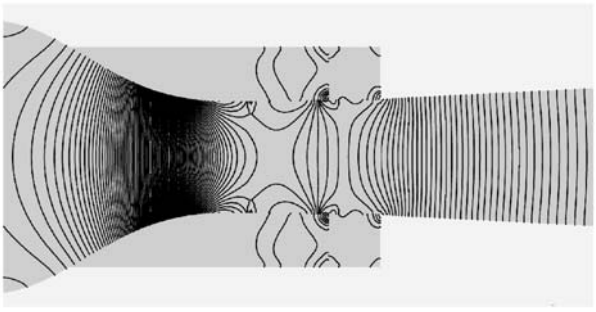

Fig. 5. Pattern of isobars in the nozzle and the diffuser of the "Struya" former.

pressure measurements in the pressure tap chamber and the mechanism of the appearance of this error are explained as follows. The measuring section following the nozzle is made expanding with a fixed opening angle of the cone of 1^{o}. This was done with the aim of compensating for the displacement thickness of the boundary layer so that the main stream of the fluid remained practically cylindrical along the full length of the measuring section with pressure tap and sampling chambers. Clearly, such a design of the nozzle and the diffuser of the "Struya" former is not optimal for all flow conditions. With one certain set of kinematic and dynamic parameters the flow remains cylindrical throughout the length of the measuring section of the diffuser, and the pressure measurement error thereby tends to zero. At any other quantities of the flow parameters (velocity, pressure, temperature, viscosity, density, etc.), a deviation from "optimality" may take place, and a diffuser with a given opening angle may not provide complete homogeneity and a flat front of the flow behind the nozzle, which leads to the appearance of insignificant (0.05–0.15%) measurement errors. The hydrodynamic nature of the initiation of this error is the presence of a "counterpressure" in the diffuser part of the measuring section, which clearly shows up as a bending of isobars (lines of equal pressures) "up the stream" (Fig. 5).

Further, the paper presents the results of the computer simulation of the influence of different characters of the inlet velocity profile on the processes of formation, mixing, and homogenization of the viscous fluid flow in the nozzle and the diffuser of the "Struya" flowmeter. Several variants of the functional dependence of the inlet velocity profile, from "mild" to "severe" nonuniformity, have been analyzed. To model the nonuniformity of the inlet velocity profile, we took, for the basis, the profile from [21] corresponding to a knee rotating by 90^{o}:

$$\frac{w}{w_0} = 0.585 + 1.64 \sin\left(0.2 + 1.95\,\frac{2y}{b_0}\right), \tag{1}$$

where w_0 is the section-average velocity; b_0 is the channel width; $-b_0/2 \le y \le b_0/2$ is the channel-height coordinate. It should be noted that formula (1) is an approximation of the experimental data for flat right knees. In the general case, as applied to the "Struya" former, we solve the three-dimensional problem (for the half-model in the presence of a vertical symmetry plane), and in the particular case where the mass forces are neglected, the former has axial symmetry. Therefore, the given functional dependence for the inlet velocity profile was used in the vertical meridian section, and for approximating the velocity profile in the horizontal direction we used the power law for a circular pipe:

$$\frac{w}{w_{\max}} = \left(1 - \frac{z}{R_0}\right)^{1/m}, \quad m \ge 1,$$

where $w_{\max}$ is the maximum velocity in the section; R_0 is the pipe radius; m is the exponent (in the calculation m = 7 was assumed); z is the coordinate in the crosswise direction.

We have simulated numerically four flows with different types of velocity profiles at the "Struya" former inlet: 1) uniform profile, $w = w_0$ = 1 m/sec; 2) "severe" nonuniformity, formula (1), $w_{\min}$ = −1.1 m/sec, $w_{\max}$ = 2.2 m/sec (a large reverse flow region at the inlet); 3) "mild" nonuniformity, modified formula (1), $w_{\min}$ = –0.1 m/sec; $w_{\max}$ = 3.2 m/sec (a small reverse flow region at the inlet); 4) weak nonuniformity, modified formula (1), $w_{\min}$ = 1 m/sec, $w_{\max}$ = 2.5 m/sec.

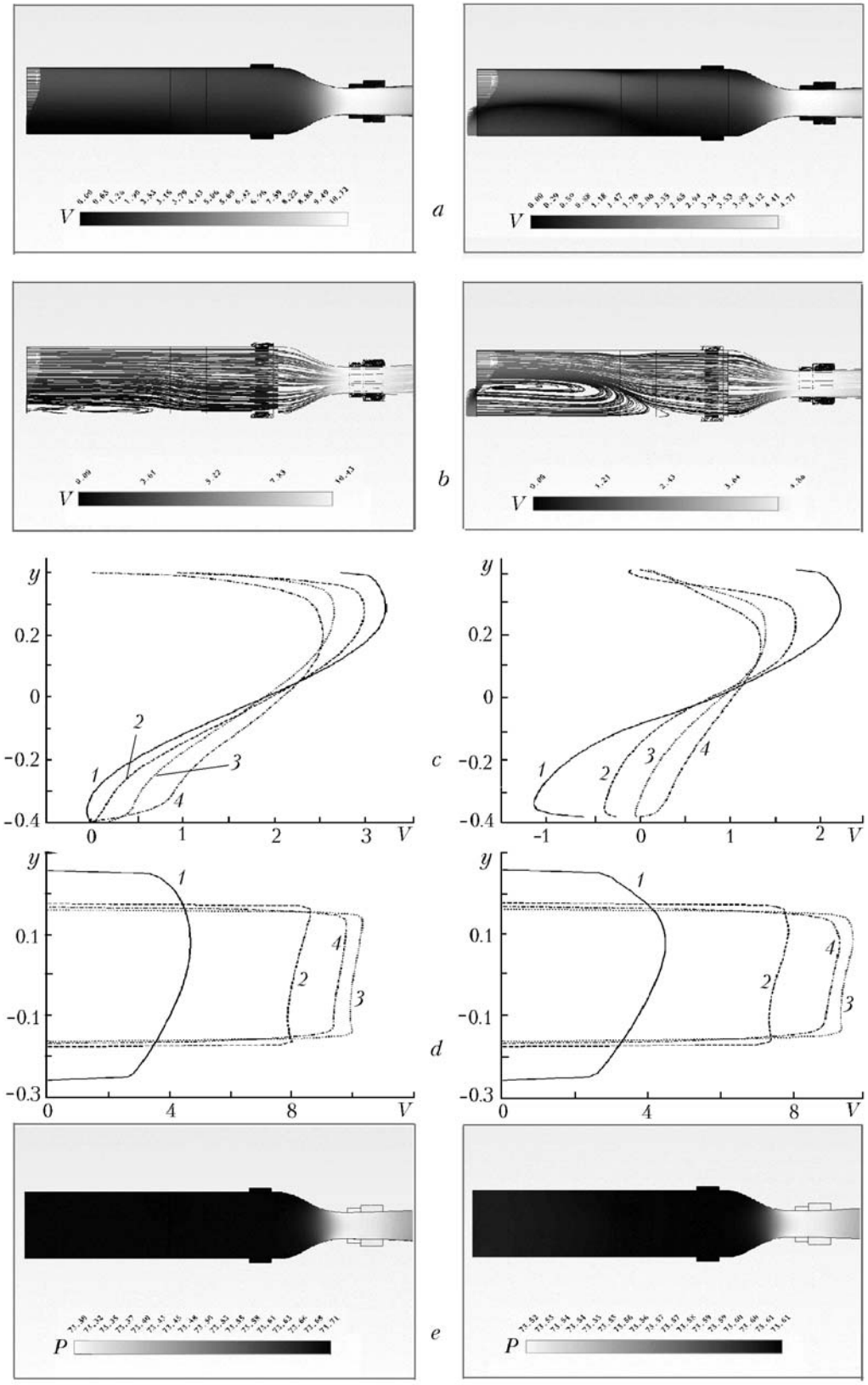
a
V
b
V
y
0.2
0
-0.2
-0.4
1
2
3
4
0
1
2
3
V
c
y
0.2
0
-0.2
-0.4
1
2
3
4
-1
0
1
2
V
y
0.1
-0.1
-0.3
1
2
3
4
0
4
8
V
d
y
0.1
-0.1
-0.3
1
2
3
4
0
4
8
V
e
P
P

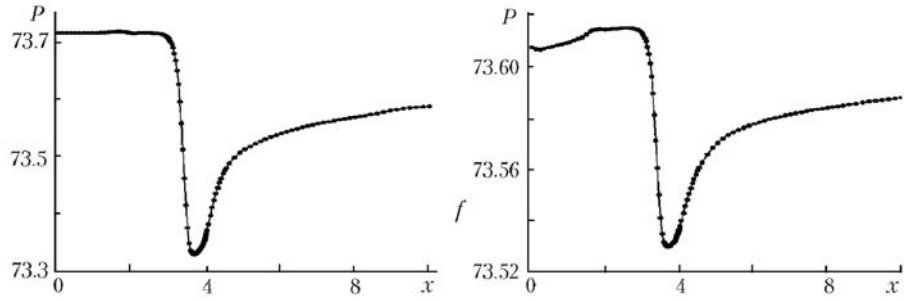

Fig. 6. Results of the numerical simulation of a homogeneous flow at the following values: ν = 200 cSt, K = 1.0 m^{-1}, ρ = 800 kg/m^3, T = 10°C, V = 1 m/sec, V_s = 1 m/sec (left column — "mild" variant of nonuniformity, right column — "severe" variant of nonuniformity): a) velocity field in the vertical symmetry plane of the former; b) streamline; c) velocity profiles before the nozzle [1) x = 0; 2) 1.6; 3) 2.0; 4) 2.8]; d) velocity profiles at the nozzle inlet, in the nozzle throat, and in the diffuser [1) x = 3.2 m; 2) 3.4; 3) 3.6; 4) 4.0]; e) pressure field; f) pressure losses along the former length. x, m; V, m/sec; P, atm.

Figure 6 illustrates the results for the regimes of "mild" and "severe" inlet nonuniformity and compares the calculated velocity distributions and patterns of streamlines in the vertical symmetry plane of the problem in the region of the nozzle, the pressure chamber, the sampling chamber, and the diffuser inlet; the velocity profiles in various sections of the inlet part, the nozzle, and the diffuser; and the distribution of hydraulic losses throughout the former channel.

Analysis of the results of the numerical simulation of the influence of different characters of the inlet velocity profile in the "Struya" former on the flow characteristics has shown that for the four different variants of the functional dependence of the velocity profile in the inlet section (from uniform with a constant velocity to nonsymmetric, strongly height-nonuniform and changing with the flow sign) the flow upon passing through the honeycomb in the working section of the nozzle and the diffuser markedly homogenizes, the "reverse" flow regions disappear, and the asymmetry of the height velocity profiles disappears.

Results of the Computer Simulation of the Dispersive Medium Flow. Simulation of multiphase inhomogeneous flows was carried out from the point of view of the model of fluid pairs (main fluid + dispersive fluid impurity). The model of fluid pairs presupposes that mixing between components occurs on scales larger than molecular scales (inhomogeneous nonuniform flows). Each fluid fraction has its own physical (density, viscosity, etc.) and hydrodynamic (velocity, temperature) parameters. Only the static pressure field is common for the components. Under the conditions of the gravitational field, for fractions of a multiphase dispersive medium having different densities, it is necessary to take into account the hydrodynamic interaction of the fractions and the processes of precipitation of dispersive impurities. Computer simulation was carried out in the ANSYS/CFX program complex on the basis of the solution of the Reynolds-averaged Navier–Stokes equations (RANS). All calculations have been made from the viewpoint of the model of a viscous incompressible dispersive fluid medium with small concentrations of the finely dispersed fluid impurity. The interphase resistance of the dispersive impurity modeled by small-diameter spherical particles was calculated by the generalized formula [22]

$$c_x = 24\left(1 + 0.15\mathrm{Re}_d^{0.687}\right)/\mathrm{Re}_d$$

obtained from the known Stokes law for small Reynolds numbers.

To obtain a steady stationary solution for each flow regime, it was necessary to carry out 200–300 iterations; for a computational grid consisting of 1 million nodes this corresponded to 10–12 h of operation of the computers.

Figure 7 shows the distributed hydrodynamic characteristics (static pressure, velocity, and turbulent kinetic energy fields, and the working pressure losses in the former channel) obtained from the viewpoint of the model of a two-phase fluid (oil) with a finely dispersed (d = 0.5 mm) water impurity (n_w = 0.5%).

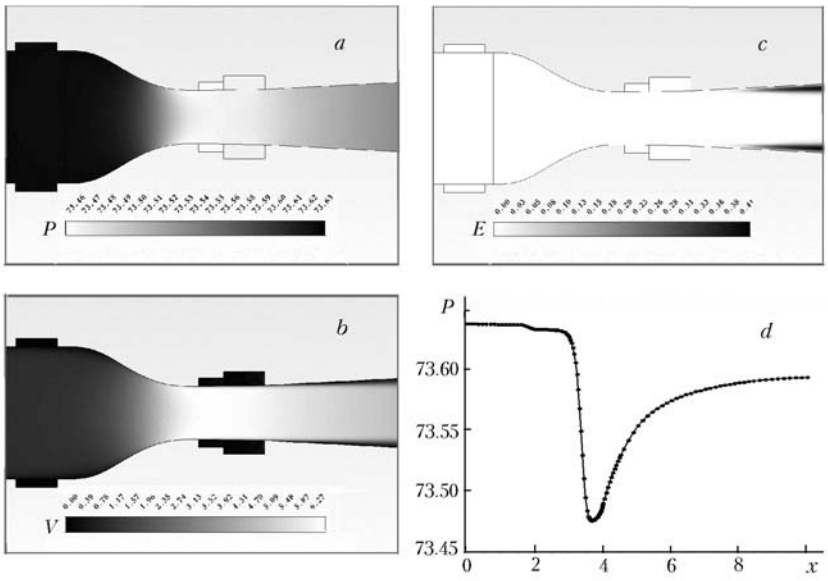

Fig. 7. Results of the numerical simulation of a dispersive fluid flow in the "Struya" former (uniform distribution of inlet mass concentrations) at the following values: ν = 200 cSt, K = 1.0 m^{-1}, ρ = 800 kg/m^3, T = 10°C, V = 1 m/sec, V_s = 1 m/sec, n_w = 0.5%, d = 0.5 mm: a) static pressure field in the vertical symmetry plane of the former; b) velocity field; c) energy field of velocity pulsations; d) pressure losses along the former length. x, m; V, m/sec; E, m^2/sec^2; P, atm.

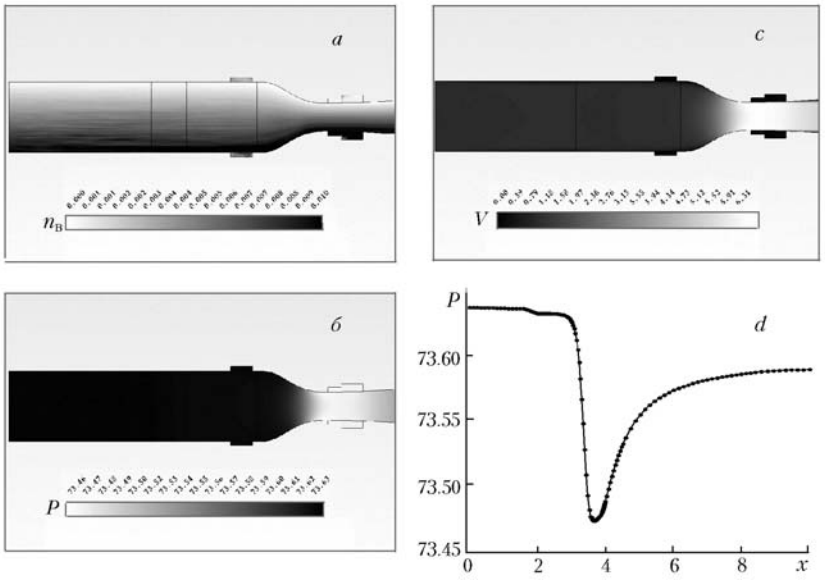

Fig. 8. Results of the numerical simulation of the two-phase dispersive fluid flow in the "Struya" former (height-linear distribution of inlet mass concentrations) at the following values: ν = 200 cSt, K = 1.0 m^{-1}, ρ = 800 kg/m^3, T = 10°C, V = 1 m/sec, V_s = 1 m/sec, n_w = 0.5%, d = 0.1 mm: a) field of volume concentrations of water in the vertical symmetry plane of the former; b) static pressure field; c) velocity field; d) pressure losses along the former length. x, m; V, m/sec; P, atm.

TABLE 1. Values of the Mass Concentrations (in fractions) of the Main Fluid and Impurity

Cross-section position	Uniform distribution		Linear distribution	
	Main fluid	Impurity	Main fluid	Impurity
Inlet cross-section	0.995000	0.005000	0.995000	0.005000
At the sampling chamber inlet	0.994971	0.005129	0.994898	0.005102
At the sampling chamber outlet	0.995063	0.004937	0.995107	0.004893

We have carried out a numerical simulation of the dispersive fluid flow in the channel of the "Struya" former for four variants of the distribution function of concentrations of the main fluid and the finely dispersed water impurity with height of the inlet section: uniform distribution, distribution linear with height, the whole of the impurity is concentrated at the top (limiting case), and the whole of the impurity is concentrated at the bottom (limiting case). Figure 8 gives, as an illustration for the performed series of calculations, the results for the most intensive and critical case of fluid flow in the "Struya" former at a fairly small Reynolds number Re = $4 \cdot 10^3$ (distribution of inlet mass concentrations linear with height). The calculations have shown that for the considered variants of distribution of concentrations of the finely dispersed impurity (water) in the main fluid (oil) at the "Struya" former inlet in the former channel, one and the same hydrodynamic flow with equal spatial distributions of the pressure, velocity, and hydraulic losses is realized. Fundamental differences are only observed in the distributions of impurity concentrations (mass fractions) with height and along the length of the former channel.

The degree of accuracy (or errors) in metrologically correct measurements of small concentrations of impurities in the fluid obtained within the framework of the calculations made can be judged from Table 1 giving the values of the mass concentrations of the main fluid and the impurity at the former inlet, the sampling chamber inlet, and at the outlet from the sampling chamber of the "Struya" former. These values have been obtained by averaging over the inlet cross-section area, the area of the narrow slots at the sampling chamber intlet, and the area of the outlet holes in the sampling chamber, respectively.

As is seen from Table 1, the possible error (at the outlet from the sampling chamber), not referred to the geometric parameters of the "Struya" former, in measuring the concentrations of the main fluid and impurities is 10^{-4} for linear concentration profiles at the "Struya" former inlet and $6 \cdot 10^{-5}$ for uniform (height-constant) concentration profiles at the inlet. The value of $6 \cdot 10^{-5}$ can be considered as the threshold minimum value of the nonreferred error of the formation of a representative sample by the "Struya" former in measuring small concentrations. Correlating the nonreferred error of the sample formation with the geometric parameters of the "Struya" former (i.e., with the ratio of the sampling cross-section to the total cross-section of the pipe) permits obtaining the referred error of the representative sample formation by the "Struya" former in measuring small concentrations, which equals 0.015 ppm for all standard sizes of the "Struya" former. This value is a threshold value in determining the limits of metrological correctness of measurements of small concentrations.

We have made calculation and theoretical estimates of the possible influence of the process of precipitation of finely dispersed fluid (water) drops contained in the mainstream (e.g., of oil) under the action of the mass forces on the results of measurements by the "Struya" former.

The equation of motion of the drop in the vertical direction in the viscous fluid flow is

$$m_{\mathrm{d}} \frac{dV_{\mathrm{yd}}}{dt} = G - A - F , \tag{2}$$

where

$$G = m_{\mathrm{d}} g ; \quad A = m_{\mathrm{d}} g \frac{\rho_{\mathrm{oil}}}{\rho_{\mathrm{w}}} ; \quad F = c_x s \rho_{\mathrm{oil}} \frac{V_{\mathrm{yd}}^2}{2} .$$

Integrating the simple differential equation (2) under the initial conditions $V_{\mathrm{yd}} = 0$ at $t = 0$, we obtain the expression for the vertical velocity of the drop:

$$V_{yd}(t) = g\frac{B}{J}\frac{1-\exp(-2BJt)}{1+\exp(-2BJt)}. \quad (3)$$

Here $B^2 = 1 - \rho_{oil}/\rho_w$; $J^2 = c_x s g \rho_{oil}/(2m_d)$. From expression (3) it is seen that the velocity of the drop reaches its maximum $V_{yd,max} = gB/J$ after an infinite time interval.

The motion of water drops of diameter of order d = 0.5–1.0 mm in the viscous fluid flow is laminar, with $\mathrm{Re}_d < 1$. The drag coefficient of the drop c_x can be estimated by the Stokes formula:

$$c_x = \frac{24}{\mathrm{Re}_d}, \quad \mathrm{Re}_d = \frac{V_{yd}d}{\nu}.$$

At the values of the parameters ρ_{oil} = 900 kg/m^3, ρ_w = 1050 kg/m^3, d = 0.5 mm, and $\nu = 50\cdot10^6$ m^2/sec the maximum velocity, of the drop is $V_{yd,max}$ = 0.5 mm/sec. Thus, estimates by the upper bound, i.e., by the velocity, show that if the passage time of the fluid flow (at a rate of 2–3 m/sec) along the channel is 1–2 sec, then water drops suspended in the main fluid have time to sink to only 1–2 d. The estimates made have shown that the process of precipitation of water drops in a viscous fluid is rather slow and does not influence the measurement data for the quality and composition of the flow in a "Struya" former having the total length of the inlet section and nozzle about 4 m.

Conclusions. The computer mathematical modeling of the fluid flow in the "Struya" flowmeter-former carried out in the ANSYS/CFX program complex has confirmed the high flowmetric characteristics of the "Struya" device.

1. Throughout the given range of variation of external parameters of the flow (working pressure, velocity, temperature) and physical parameters of the medium (fluid density and viscosity) inside the contour of the former, the pressure chamber, and the chambers for sampling, a steady fluid flow with a low level of hydraulic losses along the full length of the channel (0.06–0.35% of the working pressure) is formed.

2. The developed design of the "Struya" former makes it possible to determine with a high accuracy (0.05–0.15%) the flow core pressure in the nozzle (and, accordingly, the velocity and the flow rate of the fluid) from measurements of the static pressure in the pressure tap chamber arranged around the nozzle. The values of possible measurement errors will actually be determined only by the specifications of the measuring equipment used.

3. The "Struya" flowmeter compared to the known standard restrictions is limiting as to the achievable accuracy of differential pressure formation and is able to provide real values of the "instantaneous" error in the differential pressure formation. The existing standard restrictions either do not permit determining these vales at all or have a very high level of errors.

4. The pressure distribution pattern in the former is practically independent of the form of the inlet velocity profile, and the level of hydraulic losses throughout the channel length does not increase compared to the uniform flow conditions at the inlet. The "Struya" former provides homogenization of the velocity distribution before obtaining a uniform and section-homogeneous flow in the nozzle and the working section of the diffuser.

5. With different distributions of finely dispersed impurity (e.g., water) concentrations in the main fluid (e.g., oil) at the inlet, in the "Struya" former channel one and the same hydrodynamic flow with equal spatial pressure and velocity distributions and hydraulic losses is realized.

6. The calculation-theoretical estimates of the rate of precipitation under the action of the mass forces of finely dispersed drops of the fluid impurity (water) contained in the main fluid (oil) have shown that the processes of precipitation of water suspension in a viscous fluid are rather slow and do not influence the measurement results for the pressure, quality, and composition of the flow in the "Struya" former.

NOTATION

A, buoyancy force, N; b_0, channel width, m; c_x, aerodynamic drag coefficient of the drop; C_p, specific heat capacity, J/(kg·°C); d, drop diameter, mm; D, inlet diameter of the former; E, kinetic energy of turbulent pulsations, m^2/sec^2; F, friction force, N; g, free fall acceleration, m/sec^2; G, gravity force, N; K, loss factor in the honeycomb, m^{-1}; m, exponent; m_d, drop mass, kg; M, molar mass, kg/kmole; n_w, mass fraction of water, %; P, pressure, atm; P_{work}, working pressure, atm; R_0, pipe radius, m; $\mathrm{Re} = VD/\nu$, characteristic Reynolds number; $\mathrm{Re}_d = wd/\nu$, Reynolds number calculated by the drop diameter; s, area of the drop midsection, m^2; T, temperature, °C; t, time, sec; V, flow

velocity, m/sec; w, velocity in the channel cross-section, m/sec; w_0, cross-section-average velocity, m/sec; V_{yd}, velocity of the drop in the vertical direction, mm/sec; $V_{yd,max}$, maximum of drop precipitation, mm/sec; x, coordinate along the longitudinal axis of the former, m; y, channel-height coordinate, m; z, coordinate in the transverse direction, m; λ, heat conductivity coefficient, W/(m·°C); ν, kinematic viscosity coefficient of air, cSt; ρ, fluid density, kg/m^3. Subscripts: w, water; d, drop; oil, oil; s, sample; work, working; min, minimum; max, maximum.

REFERENCES

1. P. P. Kremlevskii, *Flowmeters and Quantity Counters* [in Russian], Mashinostroenie, Leningrad (1989).
2. *Measurement of the Flow Rate and Quantity of Liquids and Gases with the Aid of Standard Restrictions*, Pts. 1–5, GOST 8.586-2005 (ISO 5167-2003).
3. V. P. Starikov, *Flow Meter "Struya" (Jet)*, RF Patent No. 2186341, priority of 22.05.2000, published 27.07.2002, Bulletin No. 21.
4. V. P. Starikov, *Flowmeter "Struya" (Jet)*, RF Patent No. 2193756, priority of 15.08.2000, published 27.11.2002, Bulletin No. 33.
5. V. P. Starikov, Gas and liquid flowmeter "Struya" (Jet), in: *Proc. 12th Conf. "Refinement of Liquid, Gas, and Vapor Flow Rate Measurements,"* Borei-Art, St. Petersburg (2002), pp. 13–21.
6. V. P. Starikov and N. A. Vladimirova, The flowmetric characteristics of the former "Struya" (Jet): calculation of the liquid flow and hydraulic losses, in: *Proc. 24th Int. Sci.-Pract. Conf. "Commercial Metering of Energy Carriers,"* Borei-Art, St. Petersburg (2006), pp. 120–126.
7. V. P. Starikov and N. A. Vladimirova, Analysis of the influence of the inlet velocity profile on the quality of flow in the circuit of the former "Struya" and calculation of the rate of stratification of a finely dispersed liquid impurity, in: *Proc. 24th Int. Sci.-Pract. Conf. "Commercial Metering of Energy Carriers,"* Borei-Art, St. Petersburg (2006), pp. 113–119.
8. V. P. Starikov and N. A. Vladimirova, Former of a continuous representative sample on the basis of the "Struya" technology, in: *Proc. 24th Int. Sci.-Pract. Conf. "Commercial Metering of Energy Carriers,"* Borei-Art, St. Petersburg (2006), pp. 107–112.
9. V. P. Starikov and N. A. Vladimirova, The representative composition of a sample in the former "Struya" during passage of a multicomponent mixture of Newtonian fluids, in: *Proc. 25th Int. Sci.-Pract. Conf. "Commercial Metering of Energy Carriers,"* Borei-Art, St. Petersburg (2007), pp. 158–164.
10. V. P. Starikov and N. A. Vladimirova, Problems of metrological correctness of the "Struya" former (Jet), in: *Proc. 25th Int. Sci.-Pract. Conf. "Commercial Metering of Energy Carriers,"* Borei-Art, St. Petersburg (2007), pp. 149–158.
11. V. P. Starikov and N. A. Vladimirova, Precision limits of the pressure difference formation in constrictions, in: *Proc. 26th Int. Sci.-Pract. Conf. "Commercial Metering of Energy Carriers,"* Borei-Art, St. Petersburg (2007), pp. 299–305.
12. V. P. Starikov and N. A. Vladimirova, Physicochemical features of oil disperse systems and their influence on the metrological correctness and accuracy of measurements in the "Struya" former (Jet), in: *Proc. 26th Int. Sci.-Pract. Conf. "Commercial Metering of Energy Carriers,"* Borei-Art, St. Petersburg (2007), pp. 307–315.
13. V. P. Starikov and N. A. Vladimirova, Results of preliminary testing of the variable-pressure-drop flowmeter "Struya" (Jet), in: *Proc. 27th Int. Sci.-Pract. Conf. "Commercial Metering of Energy Carriers,"* Metrol. Énergosber., St. Petersburg (2008), pp. 65–79.
14. V. P. Starikov and N. A. Vladimirova, Provision of the representative sample and metrological correctness of measurements of oil disperse media, *Zavod. Labor. Diagn. Mater.*, **74**, No. 6, 75–80 (2008).
15. V. P. Starikov and N. A. Vladimirova, Metrological correctness limits of the "Struya" former (Jet), *Izmerit. Tekh.*, No. 9, 54–59 (2008).
16. N. A. Vladimirova and A. M. Sorokin, Anisotropic adaptation of three-dimensional irregular grids in problems of computational gas dynamics, *Zh. Vych. Mat. Mat. Fiz.*, **43**, No. 6, 909–919 (2003).
17. N. A. Vladimirova and A. M. Sorokin, Anisotropic adaptation of three-dimensional irregular grids in problems of computational fluid dynamics, *Comput. Math. Math. Phys.*, **43**, No. 6, 870–879 (2003).

18. N. A. Vladimirova and A. M. Sorokin, Application of anisotropic adaptation for numerical solution of two- and three-dimensional problems of gas dynamics on unstructured grids, *Aéromekh. Gaz. Dinam.*, No. 3, 21–30 (2003).
19. A. M. Sorokin and N. A. Vladimirova (O. V. Ushakova Ed.), *Anisotropic Grid Adaptation Applied to Aerodynamic Problems. Advances in Grid Generation*, ISBN 1-59454-273-2, Nova Science Publishers Inc., New York, USA (2007), pp. 189–212.
20. F. R. Menter, Two-equation eddy-viscosity turbulence models for engineering applications, *AIAA J.*, **32**, No. 8, 1598–1605 (1994).
21. I. E. Idel'chik, *Handbook on Hydraulic Resistances* [in Russian], Mashinostroenie, Moscow (1992).
22. L. Schiller and A. Naumann, *VDI Zeits.*, **77**, 318 (1933).